ELSEVIER

Thermochimica Acta 343 (2000) 89–97

thermochimica acta

www.elsevier.com/locate/tca

Latent heat measurement near a tricritical point: a study of the $KMnF_3$ ferroelastic crystal

J. del Cerro*, F.J. Romero, M.C. Gallardo, S.A. Hayward, J. Jiménez

Departmento Física Materia Condensada, Instituto Mixto Ciencia de Materiales, CSIC-Universidad de Sevilla, PO Box 1065, 41080 Sevilla, Spain

Received 22 July 1999; accepted 16 August 1999

Abstract

We present a method for measuring changes of enthalpy to discriminate the contribution due to the latent heat from that due to the temperature dependence of the specific heat near the transition point. The same conduction calorimeter, whose sensor is formed by two identical heat fluxmeters, determines the specific heat and the heat flux exchanged by the sample when its temperature changes at constant rates as low as 0.1 K h^{-1}. The method is applied to the $KMnF_3$ crystal, which undergoes a first-order transition close to a tricritical point at 186 K, and the doped crystal $KMn_{0.96}Ca_{0.04}F_3$, whose transition becomes second-order. The latent heat of pure $KMnF_3$ is evaluated to be 0.129 ± 0.002 J g^{-1}. Although the thermal analysis signal of $KMn_{0.96}Ca_{0.04}F_3$ crystal presents a peak, it is entirely due to the contribution of the specific heat, which indicates that the transition is second-order.

Keywords: Latent heat; Specific heat; Tricritical point; $KMnF_3$

1. Introduction

The crystal $KMnF_3$ presents [1] a ferroelastic phase transition from the cubic perovskite structure to a tetragonal structure at 186 K. The order parameter is related to the angle ϕ of the MnF_6 octahedral rotation around the [001] axis [2].

According to Landau classical predictions, this transition should be second-order as with $SrTiO_3$, but experimental results suggest a first-order character which might be due to anisotropic critical fluctuations [3], although its latent heat has not been measured.

Several authors [4–6] also suggest that this phase transition is close to a tricritical point. This has been confirmed by Stokka et al. [7] and Stokka and Fossheim [8], who measured the influence of the uniaxial stress on the thermal hysteresis of the transition temperature and estimated that this tricritical point is obtained when an uniaxial stress of about 0.25 kbar is applied along [100] direction.

It has been also shown that the order of this transition can be changed by substituting Ca for Mn [9–11]. The stress and doping effects are actually similar: the Ca^{++} ions are much bigger than M^{++} ions, so that they act by means of the Ca–F bond as a stress along the <001> directions of the cubic phase [10].

Because both the application of an uniaxial stress and Ca doping shift the transitions to be second-order, the $KMn_xCa_{1-x}F_3$ crystals are very appropriate for studying the critical behaviour very close to the tricritical point. To carry out this study it is necessary to measure accurately the latent heat to distinguish

* Corresponding author.

0040-6031/00/$ – see front matter
PII: S0040-6031(99)00300-7

whether, not when the transition is first- or second-order.

The measurement of latent heat very close to the tricritical point presents two difficulties: (a) the latent heat must be very small and (b) the specific heat c must show a great anomaly, for instance, the Landau theory predicts a divergence of c at the transition temperature.

On the other hand, the methods used for determining latent heat (differential scanning calorimeter, thermal analysis, etc.) really measure changes of enthalpy. This change of enthalpy has two contributions: one due to the specific heat variation with the temperature and another due to the latent heat.

There have been some attempts [12] to evaluate the first contribution from the heat flux signal when using conventional DTA in the study of samples whose specific heat has different values in each phase. Nevertheless, near a tricritical point the specific heat varies so much that we believe that this attempt is impossible unless we know separately the specific heat and the heat flux behaviours near the transition temperature.

To make heat flux and specific heat data comparable it is necessary for them to have been obtained under the same conditions. Conventional devices for measuring latent heat or specific heat work at very different temperature scanning rates. Thus, both sets of data are not completely comparable even if they have been measured using the same sample. Consequently, it is very difficult to measure latent heat very near a tricritical point with conventional devices.

We have recently built a device and developed a method which is able to measure absolute values of specific heat and heat flux exchanged by the sample under weak uniaxial stress [13,14].

The sample is pressed between two identical heat fluxmeters which are made from hundreds of thermocouples. This system can be also used as a thermal analysis device with the advantage that, due to the high number of thermocouples, its sensitivity is so high that we can use temperature scanning rates as low as $0.1\ \mathrm{K\ h^{-1}}$, which is similar to the rate used for measuring specific heat.

The sensor of the calorimeter is formed by two heat fluxmeters, two heaters and the sample. The thermal capacities and thermal resistances of these mediums have values of the same order of magnitude as the sample. On the other hand, although the temperature scanning rate can be very small, we must consider the existence of a temperature gradient in the sample and the coexistence of phases during the transition. This suggests to us the need for a revision of measurement theory, avoiding any kind of approximation in order to be able to discriminate the effect of the latent heat from that due to the temperature dependence of the thermal capacity.

In this paper, we study theoretically the heat conduction equation of a solid with temporary uniform internal dissipation and which is bounded by two parallel planes whose temperatures change at the same constant rate. The equations for the heat that crosses those surfaces are applied at the boundaries separating the different mediums forming the calorimeter, and we obtain the equations that allow us to discriminate the enthalpy variation due to the latent heat from that due to the temperature dependence of the specific heat.

This technique is applied to pure $KMnF_3$, whose latent heat is found to be $0.129 \pm 0.002\ \mathrm{J\ g^{-1}}$ and to the $KMnF_3$ crystal doped with 4% of Ca. In the case of the Ca-doped crystal, we demonstrated that, although the thermal analysis signal presents a peak at the transition temperature, this peak is entirely due to the effect of the specific heat and, consequently, the transition is second-order.

2. Heat conduction in a solid with internal source and whose temperature changes at a constant rate

Let us consider a solid bounded by two parallel planes ($x = 0,\ x = \mathrm{l}$) and we assume a linear heat conduction. The initial temperature distribution changes at a constant rate $v = (\partial/\partial t)\theta(x,t) = \text{constant}$. At the initial time ($t = 0$) a uniform time-dependent heat dissipation is produced up to time τ.

If we consider a great number N of identical time intervals u, we can approximate the above dissipation by

$$\omega(t,x) = \sum_{n=0}^{N} \omega_n (H[t-nu] - H[t-(n+1)u]), \tag{1}$$

where $Nu = \tau$, $H\,[t-nu]$ is the step function and ω_n is the power dissipated per unit volume in the interval $nu < t < (n+1)u$.

Later, at time $t_1 > Nu$, the solid attains a temperature distribution which changes at the same constant rate v,

in such a way that

$$\theta_0^1 = \theta(0, t_1) = \theta_0^0 + vt_1,$$
$$\theta_0^0 = \theta(0, 0), \quad \theta_l^1 = \theta_l^0 + vt_1. \tag{2}$$

The initial $\theta^0(x)$ and final $\theta^1(x)$ temperature distribution are, respectively,

$$\theta^i(x) = \frac{vx^2}{2h} - \frac{\dot{q}_0^i}{k}x + \theta_0^i, \quad i = 0, 1, \tag{3}$$

where h and k are the thermal diffusivity and conductivity of the solid and $\dot{q}_0^0 = \dot{q}_0^1(0, 0) = \dot{q}_0^1(0, t_1)$ are the initial and final heat fluxes through the plane $x = 0$.

Between $t = 0$ and $t = t_1$, the solution of the Laplace transform of the differential equation of heat conduction is

$$T(s,x) = L[\theta(t,x)] = A\,\mathrm{e}^{x(s/h)^{1/2}} + B\,\mathrm{e}^{-x(s/h)^{1/2}} + \sum_{n=0}^{N}\omega_n\frac{(\mathrm{e}^{-snu} - \mathrm{e}^{-s(n+1)u})}{\rho c s^2} + \frac{v}{s^2} + \frac{\theta^0(x)}{s}, \tag{4}$$

where ρ and c are the density and specific heat of the solid and A and B are constants. From the above equation we can relate the Laplace transforms of temperature T_0, T_l and the transform of heat fluxes I_0, I_l at the boundaries $x = 0$ and $x = l$, respectively,

$$\begin{bmatrix} (I_0 - \dot{q}_0^0/s)(sk\rho c)^{-1/2} \\ (I_l - \dot{q}_l^0/s)(sk\rho c)^{-1/2} \end{bmatrix} = \begin{bmatrix} \coth(l(s/h)^{1/2}) - \mathrm{cosech}(l(s/h)^{1/2}) \\ \mathrm{cosech}\,(l(s/h)^{1/2}) - \coth(l(s/h)^{1/2}) \end{bmatrix} \times \begin{bmatrix} (T_0 - \theta_0^0/s - \phi). \\ (T_l - \theta_l^0/s - \phi) \end{bmatrix}, \tag{5}$$

$$\phi = \sum_{n=0}^{N}\omega_n\frac{(\mathrm{e}^{-snu} - \mathrm{e}^{-s(n+1)u})}{\rho c s^2} + \frac{v}{s^2}.$$

Using coth and cosech series and integration by parts, from Eq. (5) we obtain,

$$\frac{l}{k}I_0 = (T_0 - T_l) + \frac{vl^2}{2hs} + \alpha\big[s(T_0 + T_l) - (\theta_0^0 + \theta_l^0) - 2s\phi\big] + \beta\big[s(T_0 - T_l) - (\theta_0^0 - \theta_l^0)\big], \tag{6}$$

$$\alpha = \sum_{m=0}^{\infty}\frac{2l^2/h}{(2m+1)^2\pi^2 + l^2 s/h},$$
$$\beta = \sum_{m=0}^{\infty}\frac{2l^2/h}{(2m\pi)^2 + l^2 s/h}.$$

The Laplace integrals can be expressed as

$$\int_0^{\infty} f(t)\mathrm{e}^{-st}\,\mathrm{d}t = \int_0^{t_1} f(t)\mathrm{e}^{-st}\,\mathrm{d}t + \int_{t_1}^{\infty} f^1\mathrm{e}^{-st}\,\mathrm{d}t, \quad f^1 = f(t \geq t_1).$$

Then, from Eq. (6) and considering Eqs. (2) and (3) we can deduce

$$\frac{l}{k}\int_0^{t_1}\dot{q}_0\,\mathrm{e}^{-st}\,\mathrm{d}t = \int_0^{t_1}(\theta_0 - \theta_l)\mathrm{e}^{-st}\,\mathrm{d}t + \frac{v}{2}\left(\frac{l^2}{h} - 4\alpha\right)\int_0^{t_1}\mathrm{e}^{-st}\,\mathrm{d}t + \alpha\int_0^{t_1}\mathrm{e}^{-st}\,\mathrm{d}(\theta_0 + \theta_l) + \beta\int_0^{t_1}\mathrm{e}^{-st}\,\mathrm{d}(\theta_0 - \theta_l) - 2\alpha\int_0^{Nu}\sum_{n=0}^{\infty}\frac{\omega_n}{\rho c}(H[t - nu] - H[t - (n+1)u])\mathrm{e}^{-st}\,\mathrm{d}t. \tag{7}$$

As the above integrals converge, we consider the limit $s \to 0$. As $\alpha(s = 0) = l^2/(4h)$ and $\beta(s = 0) = l^2/(12h)$ we obtain

$$\int_0^{t_1}\dot{q}_0\,\mathrm{d}t = q_0 = \frac{k}{l}\int_0^{t_1}(\theta_0 - \theta_l)\,\mathrm{d}t + \rho c l\left[\frac{\theta_0^1 - \theta_0^0}{3} + \frac{\theta_l^1 - \theta_l^0}{6}\right] - \frac{l}{2}\sum_{n=0}^{N}\omega_n u. \tag{8}$$

As $\theta_0^1 - \theta_0^0 = \theta_l^1 - \theta_l^0 = vt_1$, if we multiply by the section S of the solid, we deduce

$$Q_0 = \int_0^{t_l}\frac{\theta_0 - \theta_l}{R}\,\mathrm{d}t + \frac{C}{2}vt_1 - \frac{Q}{2}, \tag{9}$$

where Q_0 is the total heat that has crossed the plane $x = 0$ between 0 and t_1, R and C are the thermal resistance and thermal capacity of the solid and Q is the total heat dissipated in the solid.

Similarly from Eq. (5) we deduce that the total heat Q_l which has passed through plane $x = l$ between $t = 0$ and $t = t_1$ is

$$Q_l = \int_0^{t_l}\frac{\theta_0 - \theta_l}{R}\,\mathrm{d}t - \frac{C}{2}vt_1 + \frac{Q}{2}. \tag{10}$$

We must point out that these equations do not depend on the time dependence of the dissipation. Obviously, Eqs. (9) and (10) are fulfilled in simple situations, for instance, when there is no dissipation in the solid, then $Q = 0$ in Eqs. (9) and (10).

3. Measurement of latent heat by means of fluxmeters

The experimental arrangement of the specific heat measurement was described previously in detail by Gallardo et al. [13] and is represented in Fig. 1.

The sample is pressed between two identical heat fluxmeters which are made from 50 chromel–constantan thermocouples [15] connected in series with the wires placed in parallel lines. One of the fluxmeters is fixed to a calorimeter block while the other is pressed by a bellows. The fluxmeters which have a cross-section of 1 cm^2, are rigid enough to apply a controlled uniaxial stress of between 0 and 12 bars on the sample. Two electrical resistances (heaters) are placed between each face of the sample and fluxmeters. These resistances can dissipate a uniform heat power on the sample faces or measure the temperature of the fluxmeter junctions near the sample.

An HPE-1328A current source and a HPE-l326 multimeter are used, respectively, to produce and to measure the power dissipated in the heaters. The e.m.f. produced by the fluxmeters is measured by a Keithley 181 nanovoltmeter with a repetition rate of four measurements per second. The temperature of the calorimeter block is measured with a platinum resistance thermometer and a Tinsley resistance bridge. All the devices are controlled by an HP-75000 data acquisition system.

To measure the latent heat, we change the temperature of the calorimeter at a low constant rate ($v \cong 0.1\ K\ h^{-1}$) so that in every medium (fluxmeter, heater and sample) the initial conditions considered in Section 2 are present. Due to the symmetry of the assembly, the high vacuum in the calorimeter and the small temperature difference between the sample and the block (which is estimated to be lower than 0.02 K) we can assume a linear heat conduction in each medium.

When the temperature of the sample surface in contact with the heater reaches the transition temperature the change of phase begins and we assume that the propagation front of the phase transition coincides with the planes $x =$ constant and there is no heat flux through the symmetry plane $x = 0$ of the sample (Fig. 1).

If the phase transition is completed at a time τ and like the thermal capacity of the block is much higher than that of the sample, at time $t_1 > \tau$ a new uniform temperature distribution is reached where the temperature in every medium changes at the same rate v, thus obtaining the final conditions described in Section 2.

Now, we consider the following model:

The sample is composed by $2N$ thin slabs (where N is large). The width of these slabs is so small that we assume that the transition within each slab occurs uniformly. In Fig. 2, we show the assembly described above where the fluxmeter, the heater and the N slabs

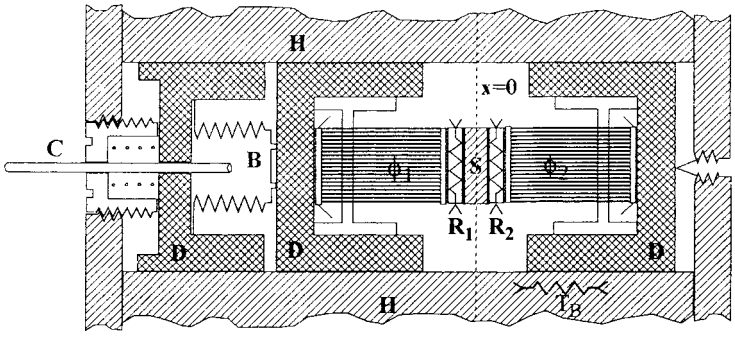

Fig. 1. Diagram of the sensor: Φ_1 and Φ_2 — heat fluxmeters, R_1 and R_2 — heaters, S — sample, B — bellow, D — fluxmeters and bellow container, H — heat sink, and C — capillary.

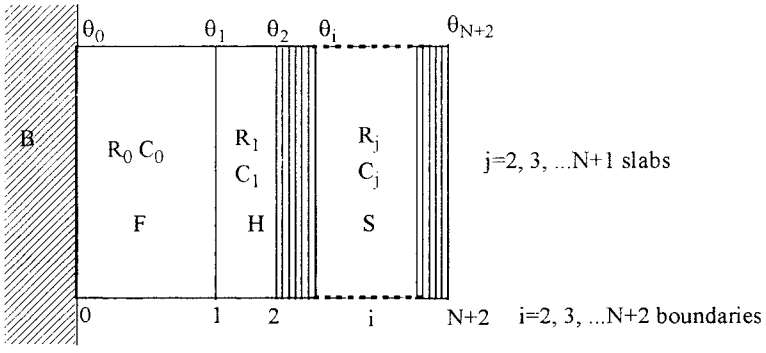

Fig. 2. Design of the device: (B) calorimeter block, (F) fluxmeter, (H) Heater and (S) sample which consist of N thin slabs where the phase transition is produced uniformly. R_j, C_j where $j = 0, 1, \ldots, N+1$ are the thermal resistance and thermal capacity of each medium and θ_i is the temperature at the boundaries where $i = 1, 2, \ldots, N+1$.

are represented by mediums 0, 1, 2, …, $N+1$, respectively. Due to symmetry we consider there is no heat flux through boundary $N+2$.

The slabs transform sequentially from $i = 2$ at the initial time to medium $i = N+1$. In this model the latent heat is equivalent to a positive or negative internal dissipation. Thus, if we consider a time t_1 high enough to re-establish the initial temperature variation rate at every point of the assembly, we can apply Eqs. (9) and (10) at the boundaries 1, 2,…, $N+1$ of Fig. 2.

$$\int_0^{t_1} \frac{\theta_i - \theta_{i+1}}{R_i}\,\mathrm{d}t - \frac{C_i}{2}vt_1 + Q_i = \int_0^{t_1} \frac{\theta_{i+1} - \theta_{i+2}}{R_{i+1}}\,\mathrm{d}t + \frac{C_{i+1}}{2}vt_1 - Q_{i+1}$$

$$\text{for } i = 0, 1, \ldots, N \text{ with } Q_0 = Q_1 = 0,$$

where C_i and R_i are the thermal capacity and thermal resistance of each medium. Because of the symmetry of the assembly, we assume that there is no heat flux through the boundary $N+2$,

$$\int_0^{t_1} \frac{\theta_{N+1} - \theta_{N+2}}{R_{N+1}}\,\mathrm{d}t - \frac{C_{N+1}}{2}vt_1 + Q_{N+1} = 0.$$

From the above equation we obtain,

$$\int_0^{t_1} \frac{\theta_0 - \theta_1}{R_0}\,\mathrm{d}t = \left[\frac{C_0}{2} + C_1 + \sum_{i=2}^{N+1} C_i\right] vt_1 - \sum_{i=2}^{N+1} Q_i = -\frac{1}{\alpha}\int_0^{t_1} V\,\mathrm{d}t, \tag{11}$$

where we have used the Seebeck law $V = n\epsilon(\theta_1 - \theta_0)$ at the fluxmeter and its sensitivity $\alpha = n\epsilon R_0$ which is determined by calibration of Eq. (13). V is the e.m.f. given by the fluxmeter, n the number of thermocouples and ϵ is the Seebeck coefficient.

We consider now two cases:

(a) When there is no phase transition, $\sum_{i=2}^{N+1} Q_i = 0$ in Eq. (11) and $\sum_{i=2}^{N+1} C_i = C_S$ is the thermal capacity of the half of the sample. In this case, each point of the assembly changes at the same constant rate v. Since the relaxation time of the fluxmeter is lower than 2 min and the rate v is very small ($v \cong 0.1\ \mathrm{K\,h^{-1}}$), we can consider a small interval of time in such a way that we can assume the thermal capacities and the e.m.f. V are practically constant and consequently we deduce

$$V = -\alpha v(C_F + C_S), \tag{12}$$

where $C_F = \frac{C_0}{2} + C_1$. If V and C_S are measured, α and v are known and C_F is evaluated as we will see below. Eq. (12) must be fulfilled in the temperature ranges where there is no contribution from the latent heat.

(b) During the time interval 0–t_1, the first-order transition is produced. In this case $\sum_{i=2}^{N+1} Q_i = (m/2)\Delta h$ where m is the mass of the sample and Δh is its latent heat.From Eq. (11)

$$\frac{1}{\alpha}\int_0^{t_1} V\,\mathrm{d}t = \frac{m}{2}\Delta h - \left(C_F + \sum_{i=2}^{N+1} C_i\right) vt_1. \tag{13}$$

This equation shows that the total change of enthalpy (measured by the integral of the DTA signal) is the

change of enthalpy due to the latent heat plus that due to thermal capacities. As we will see below this equation allows us to determine the latent heat.

4. Experimental results

We have studied a pure $KMnF_3$ crystal and a doped $KMn_{0.96}Ca_{0.04}F_3$ crystal, both 5 mm thick and with a cross-section of 0.8 mm^2. They were grown using the Bridgman–Stockbarger technique.

The specific heat of both crystals was measured using the method previously described [13]. The same constant power was dissipated in both heaters (Fig. 1) for 10 min to reach a steady state. Then the power was cut off and the e.m.f. V of the fluxmeters was integrated for another period of 10 min. The integration of this e.m.f. V allows us to determine the thermal capacity of the sample. Then, the power was switched on again and the sequence was continuously repeated while the temperature of the sample was cooled at a low constant rate of 0.06 K h^{-1}.

In Fig. 3, data of both crystals are represented against temperature in a small range covering both transitions. As with previous results [11], we can see that the transition temperature T_{tr} shifts from 186 K for a pure crystal to 200.5 K for the doped crystal and the specific heat behaviour is very different in both cases. A complete analysis of both sets of data is in progress and we will report it in a forthcoming paper.

On the other hand, according to the method developed in the previous sections, the latent heat of the sample can be determined using the equipment as a very sensitive DTA device: the calorimeter block was cooled and heated at the same constant rate used for the measurement of the specific heat (0.06 K h^{-1}) and also at 0.16 K h^{-1}. The e.m.f. V given by the fluxmeters was continuously measured without heat dissipation in any heater.

In Figs. 4 and 5, we represent the e.m.f. V versus temperature T of the block for the doped and pure crystal, respectively, obtained when cooling at 0.16 K h^{-1}. With conventional DTA, the latent heat is calculated by integrating V with respect to an appropriate base line V^0. Nevertheless, if we observe both figures, V is different below and above the

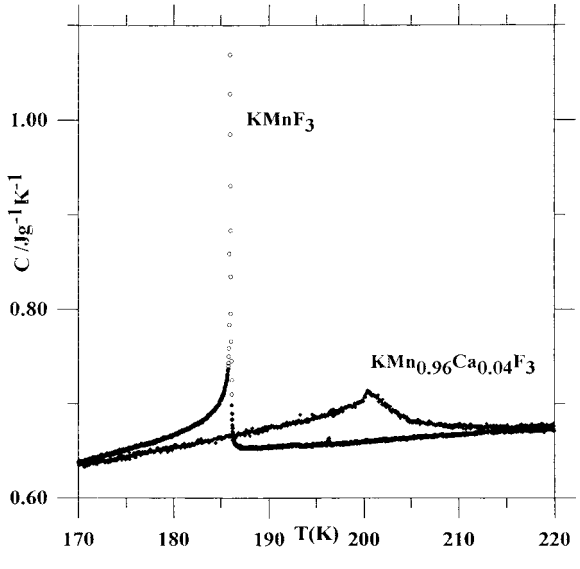

Fig. 3. Specific heat of pure $KMnF_3$ (●) and $KMn_{1-x}Ca_xF_3$ (◆) versus temperature near their transition points. We also represent the specific heat data of pure $KMnF_3$ (○) affected by the latent heat.

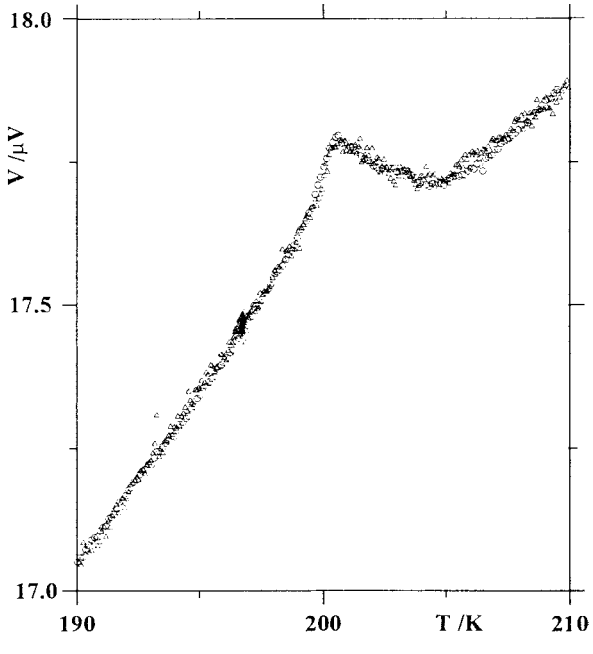

Fig. 4. Measured V (○) and calculated V_c (Δ) versus temperature of the block when cooling the $KMn_{0.96}Ca_{0.04}F_3$ crystal at 0.16 K h^{-1}. For clarity, only every 20th measured point of V is shown.

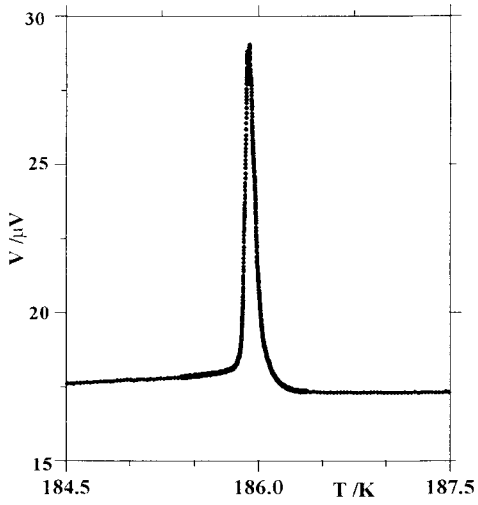

Fig. 5. Measured V (●) versus temperature of the block when cooling the $KMnF_3$ crystal at 0.16 K h^{-1}. The greater thickness of the curve close to the transition point is due to the higher reading rate of V.

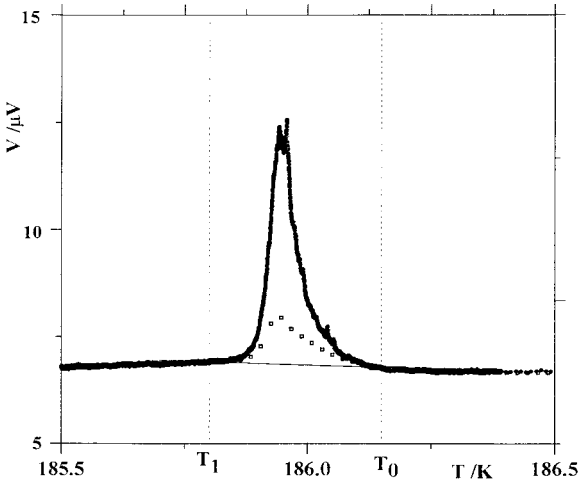

Fig. 6. Measured V (●) and calculated V_c (□) versus temperature of the block when cooling the $KMnF_3$ crystal at 0.06 K h^{-1}. (T_0, T_1) is the range where V and V_c do not coincide. The straight line between $V(T_0)$ and $V(T_1)$ which is the appropriate baseline is also shown.

transition point and, mainly, it changes continuously with temperature in such a way that we cannot know when the transition begins or ends by considering only these data. It is impossible to evaluate the baseline V^0 only from the e.m.f. V data. We proceed as follows:

From specific heat data C_S (represented in Fig. 3) and e.m.f data V (represented in Figs. 4 and 5), we consider the values of C_S and V at two different temperatures, where we assume there is no effect from the latent heat, above and below the temperature T_m of the maximum value of V (for the doped and pure crystals we have considered, respectively, 5 and 1 K above and below it). Using these data in Eq. (13) we evaluate the term C_F at those temperatures. In this temperature range, there is no anomaly in the thermal capacity of both fluxmeter and heater, thus, we can assume a linear temperature dependence of C_F in this small temperature range.

Now, using this linear relation together with specific heat data of the sample in that temperature range, Eq. (12) allows us to calculate the e.m.f. V_c, that according to the theory is due exclusively to the thermal capacity behaviour. Comparing the measured V and the calculated V_c we deduce that in the temperature range where both e.m.f. coincide there is no effect from latent heat. The temperature dependence of V_c obtained for doped crystals is also represented in Fig. 4 and that corresponding to the pure crystal is represented in small range of temperature in Fig. 6.

We can observe that for the doped crystal (Fig. 4) V and V_c coincide over the entire temperature range, thus showing that the change of enthalpy is due exclusively to the specific heat anomaly. This confirms that the transition at 200 K in $KMn_{0.96}Ca_{0.04}F_3$ crystal is second-order [11]. The fact that V and V_c coincide at temperatures outside of 5 K around the transition point can be considered as a proof of the validity of the method.

In Fig. 6, we represent V obtained when cooling the pure $KMnF_3$ at $v = -0.06$ K h^{-1} and the calculated V_c versus temperature of the block. We must point out that, according to Eq. (12), V is proportional to v. If we compare the ratio V/v for $v = -0.16$ K h^{-1} (Fig. 5) and $v = -0.06$ K h^{-1} (Fig. 6), we obtain a good agreement of both data (the discrepancy is less than 1%). This can be considered as another proof of the validity of this procedure.

From Fig. 6, we can observe that V and V_c only coincide for $T < T_1 = 185.80$ K and $T > T_0 = 186.15$ K. As above, the variation of enthalpy outside the temperature interval (T_1, T_0) is due exclusively to the variation of the specific heat with temperature. In the temperature range $\Delta T = T_0 - T_1$, V and V_c are different thus showing the existence of a latent heat.

In other words, the temperature dependence of the heat flux observed for $T < T_1$ and $T > T_0$ is due exclusively to the specific heat anomaly close to the transition point while data observed between T_0 and T_1 are due to both, the specific heat and latent heat. The main advantage of this method is the clear determination of the block temperature range $T_1 - T_0$ between which the phase transition is produced with coexistence of both phases. As T changes linearly with time, this allows us to know the time interval t_1, (Eq. (13)), during which the phase transition is produced.

According to the usual procedure in DTA and DSC techniques, we can consider the straight line $V(T_0) - V(T_1)$ as the baseline to evaluate the latent heat. Nevertheless, we are going to discuss several points justifying the above procedure:

- The specific heat and the V data are represented versus the block temperature T. Generally, the temperature of the sample boundary T_s changes at the same rate v as the block although with a delay evaluated in 0.005 K (temperature difference between the ends of fluxmeters). Nevertheless, during the coexistence of both phases and due to the latent heat effect, T_s does not change at the same rate v and it can even remain practically constant if the latent heat is high enough. In other words, the temperature range where both phases coexist is much smaller than $T_0 - T_1$.
- In the coexistence interval $T_1 - T_0 = 0.35$ K, specific heat data are affected by latent heat during the measurement process, so they are higher than the true ones. These data are shown as open circles in Fig. 3. The filled circles represent the singular behaviour of the specific heat near the phase transition and they are outside of $T_1 - T_0$ so they are not affected by the latent heat.
- The change of phase is completed in about 2.5 h when $v = 0.16$ K h^{-1} and 6 h when $v = 0.06$ K h^{-1} while the relaxation time of the fluxmeters is about 2 min.

When cooling, at block temperature T_0 ($t = 0$) the ferrophase begins to appear while at T_1 ($t = t_1$) we can consider that the first-order transition has finished. Then $C(T_0)$ and $C(T_1)$ are the specific heats of saturated paraphase and saturated ferrophase, respectively. During the interval t_1 there is coexistence of both phases whose properties depend on the molar fraction X. Consequently, the thermal capacity contribution to heat flux depends on X too. It is necessary to assume that due to the very small temperature scanning rate the change of phase is produced uniformly between $X = 0$ and $X = 1$. In other case, we cannot evaluate the baseline.

Table 1
Latent heat of pure $KMnF_3$ for several cooling and heating rates

v (K h^{-1})	L (J g^{-1})
−0.06	0.129
−0.16	0.126
+0.06	0.129
+0.18	0.130

This assumption means that in Eq. (13) $\Sigma C_i = m[c(T_0)X + c(T_1)(1 - X)]$, i.e., that ΣC_i changes linearly with t between $mc(T_0)$ and $mc(T_1)$ and consequently the thermal capacity contribution in Eq. (13) is the area of the trapezium formed by the straight line between $V(t = 0)$ or $V(T_0)$ and $V(t = t_1)$ or $V(T_1)$, respectively.

The above assumption seems very reasonable and in the case of other nonuniform kinetics, the error produced considering the straight line must be very small because necessarily the baseline goes from $V(T_0)$ to $V(T_1)$ by a line which must not be very different from the straight line.

The crucial point of the procedure developed in this paper is the determination of the temperature range $T_0 - T_1$ where the first-order transition is produced and DTA trace changes strongly with temperature due to the specific heat anomaly.

In summary, the latent heat is determined by integrating V respect to the straight line $V(T_0) - V(T_1)$.

Using this procedure, the values obtained for cooling and heating the sample at 0.06 and 0.16 K h^{-1} are given in Table 1, showing very good reproducibility.

We must insist that in the doped crystal (Fig. 4) it would have been impossible to determine the base line if we had not used this procedure. In this case $T_0 - T_1 = 0$, so the transition is second-order.

5. Conclusions

The method we have developed allows us to discriminate the changes of enthalpy due to the specific

heat variation with temperature from that due to the latent heat. It determines clearly the interval where the latent heat is produced and the baseline with respect to which the DTA signal should be integrated.

The theory is quite general and it has been developed to show that the measurement does not depend on the thermal properties of sample and sensor. It includes also that the change of phase is produced gradually and there is no dependence from temperature gradients in the sample.

The method presents the following main advantages:

1. Due to the high number of thermocouples and the great thermal stability of the calorimeter block, the device has a high sensitivity and we can carry out cooling and heating runs at extremely low constant rates. This minimises the temperature gradients in the sample.
2. The thermal capacity and the enthalpy changes can be measured on the same sample, with the same device and at similar thermal conditions. The comparison of both sets of data allows us to correctly determine the base line with respect to which the integration of heat flux should be carried out and, consequently, to evaluate the latent heat of the sample. This advantage is very important for studying samples close to a tricritical point where the latent heat is small and the specific heat changes greatly with the temperature near the transition point. We must point out that in this case the DTA signal changes continuously and it is impossible to know the temperature interval where the latent heat is produced unless we use specific heat data.
3. Measurements carried out upon heating and cooling the sample at two different temperature variation rates show a very good reproducibility, allowing us to evaluate the latent heat of pure $KMnF_3$ as 0.129 ± 0.002 J g^{-1}.
4. We can discriminate the specific heat data affected by the latent heat during the measurement process.
5. With this equipment it is possible to apply a uniaxial stress [16] or an electric field on the sample to see its effect on the latent heat or on the specific heat and to study its effects on the transitions. Measurements of the latent heat of $KMnF_3$ under different small uniaxial pressures are also in progress.

Measurements with $KMnF_3$ samples with smaller percentage of doping are now in progress with the goal of studying the specific heat behaviour of first- and second-order transitions even closer to the tricritical point.

Acknowledgements

We are grateful to A. Gibaud and Ph. Daniel for growing the samples. This work has been supported by Project PB95-0546 of Spanish DGICYT and by the TMR network ‘‘Mineral Transformations’’ No. ERB-FMRX-CT97-0 108.

References

[1] V.J. Minkiewicz, Y. Fujii, Y. Yamada, J. Phys. Soc. Jpn. 28 (1970) 443.
[2] R.A. Cowley, Adv. Phys. 29 (1980) 1.
[3] A. Aharony, Ferroelectrics 24 (1980) 313.
[4] H. Sakashita, N. Ohama, A. Okazaki, J. Phys. Soc. Jpn. 50 (1981) 4013.
[5] H. Sakashita, N. Ohama, A. Okazaki, Phase Transitions 28 (1990) 99.
[6] U.J. Nicholls, R.A. Cowley, J. Phys. C 20 (1987) 3417.
[7] S. Stokka, K. Fossheim, V. Samulionis, Phys. Rev. Lett. 47 (1981) 1740.
[8] S. Stokka, K. Fossheim, J. Phys. C 15 (1982) 1161.
[9] U.J. Cox, A. Gibaud, R.A. Cowley, Phys. Rev. Lett. 61 (1988) 982.
[10] A. Gibaud, R.A. Cowley, J. Nouet, Phase Transitions 14 (1989) 129.
[11] A. Gibaud, S.M. Shapiro, J. Nouet, H. You, Phys. Rev. B 44 (1991) 2437.
[12] E.Y. Ding, X.H. Liang, Thermochim. Acta 323 (1998) 93.
[13] M.C. Gallardo, J. Jiménez, J. del Cerro, Rev. Sci. Instrum. 66 (1995) 5288.
[14] M.C. Gallardo, J. Jiménez, M. Koralewski, J. del Cerro, J. Appl. Phys. 81 (1997) 2584.
[15] J. Jiménez, E. Rojas, M. Zamora, J. Appl. Phys. 56 (1984) 3353.
[16] M.C. Gallardo, J. Jiménez, J. del Cerro, E.K.H. Salje, J. Phys.: Condens. Matter 8 (1996) 85.